Correlation differences in heartbeat fluctuations during rest and exercise

Roman Karasik,[1] Nir Sapir,[1] Yosef Ashkenazy,[2] Plamen Ch. Ivanov,[3,4] Itzhak Dvir,[5] Peretz Lavie,[6] and Shlomo Havlin[1]
[1]*Department of Physics and Gonda-Goldschmied Medical Diagnostic Research Center, Bar-Ilan University, Ramat-Gan 52900, Israel*
[2]*Center for Global Change Science, Massachusetts Institute of Technology, MIT Room 54-1726, Cambridge, Massachusetts 02139*
[3]*Center for Polymer Studies and Department of Physics, Boston University, Boston, Massachusetts 02215*
[4]*Beth Israel Deaconess Medical Center, Harvard Medical School, Boston, Massachusetts 02215*
[5]*Itamar Medical Ltd., Cesarea, Israel*
[6]*Sleep Laboratory, Faculty of Medicine, Technion-Israel Institute of Technology, Haifa, Israel*
(Received 11 October 2001; revised manuscript received 20 September 2002; published 12 December 2002)

We study the heartbeat activity of healthy individuals at rest and during exercise. We focus on correlation properties of the intervals formed by successive peaks in the pulse wave and find significant scaling differences between rest and exercise. For exercise the interval series is anticorrelated at short-time scales and correlated at intermediate-time scales, while for rest we observe the opposite crossover pattern—from strong correlations in the short-time regime to weaker correlations at larger scales. We also suggest a physiologically motivated stochastic scenario to provide an intuitive explanation of the scaling differences between rest and exercise.

DOI: 10.1103/PhysRevE.66.062902 PACS number(s): 87.19.Hh, 05.45.Tp, 89.75.Da

One of the important questions in the analysis of complex physiological time series is how such series reflect the dynamical properties associated with the underlying control mechanism [1,2]. Recently, it was found, e.g., that the fluctuations of the heart interbeat intervals reveal long-range power-law correlations [3] and follow scale-invariant structure [4] which may be useful for diagnosis and prognosis [5]. Here we study the correlation (scaling) properties of heartbeat dynamics as reflected by the pulse wave measured from the finger [6,7].

Previous studies of interbeat interval series have focused primarily on long records of at least several hours [8,9], which include periods of rest as well as periods of a more intensive physical activity. However, heartbeat dynamics can change dramatically with physical activity. Thus, important differences in cardiac regulation associated with rest and exercise may not be clearly seen when analyzing records which mix together rest and exercise regimes. Here we consider rest and exercise activities *separately*. We focus on the correlations in the interpulse interval (IPI) series derived from the pulse wave signal during rest and exercise [Fig. 1(a)]. By studying the changes in the correlation properties we wish to achieve a better understanding of the physiological mechanism that regulates heartbeat dynamics at rest and during physical exercise.

We analyze 21 records from healthy subjects. Each record includes four different stages of physical activity denoted as *rest 1*, *exercise 1*, *rest 2* and *exercise 2* [Fig. 1(b)]. At the first stage (*rest 1*) we measure the IPI under normal rest conditions. At the next stage (*exercise 1*) subjects are asked to run on a treadmill. After a short *recovery*, during which subjects sit down to recover their heart rate, a new rest-exercise episode (denoted as *rest 2* and *exercise 2*) is followed.

To study the correlation properties of the IPI series, we use the detrended fluctuation analysis (DFA) [10] which is a method developed to avoid spurious detection of correlations that are artifacts of trends related to nonstationarity. The DFA procedure consists of the following steps. We first integrate the IPI series $\{u_i\}$ to construct the profile $Y(k)=\Sigma_{i=1}^{k}(u_i-\langle u\rangle)$, where $\langle u\rangle$ is the series average. Next, we divide the integrated series $Y(k)$ into equal nonoverlapping windows of size n and find the local trend in each window by a least-squares polynomial fit. The order of the polynomial fit specifies the order of the DFA [11,12]. Then we calculate the average of the square distances around the local trend. This procedure is repeated to obtain the root mean square fluctuation function $F(n)$ for different window sizes n. A power-law relation $F(n)\sim n^{\alpha}$ indicates the presence of scaling in the series. According to random walk theory, the scaling exponent α is related to the autocorrela-

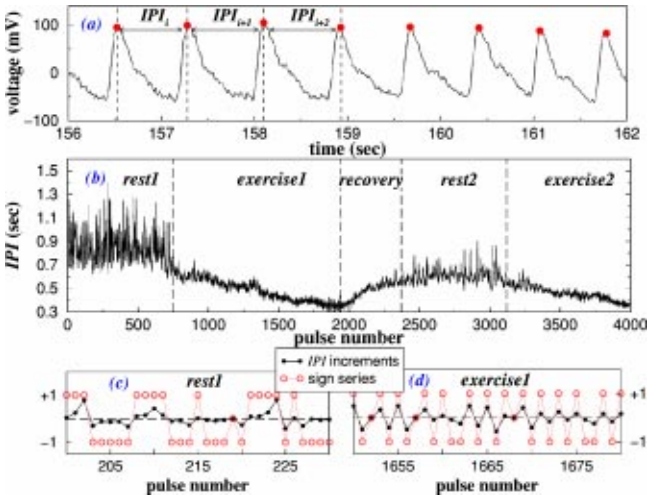

FIG. 1. (a) A typical example of a pulse wave measured as a function of time. As in the case of the electrocardiogram signal where interbeat interval fluctuations are studied (see, e.g., Ref. [8]), we analyze the interpulse intervals (IPIs) between successive peaks in the pulse wave. (b) IPI series obtained from the pulse wave signal shown in (a). Each record includes two rest and two exercise stages. The duration of each stage varies from subject to subject and is between 6 and 10 min. (c) Sign series obtained from the increments in the interpulse intervals during rest and (d) during exercise. Note that the sign series of the exercise regime exhibits more frequent alternations (stronger anticorrelated behavior) compared to rest.

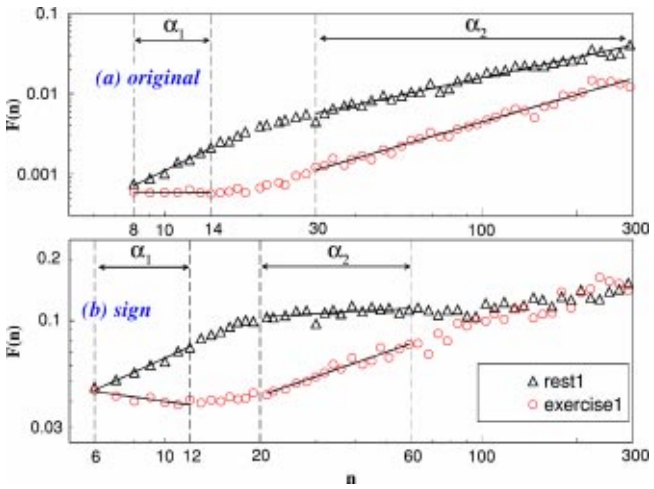

FIG. 2. Fluctuation function *F(n)* as a function of time scale *n* (in pulse number) for rest (Δ) and exercise (○) stages of a typical healthy subject for (a) the original IPI series and (b) the sign series of the IPI increments. For all records we observe a crossover between two different regimes of correlations. The dashed lines indicate the boundaries of these regimes in which short-range scaling exponents α_1 and intermediate exponents α_2 have been calculated. Note the different crossover patterns for rest ($\alpha_1 > \alpha_2$) and exercise ($\alpha_1 < \alpha_2$) stages.

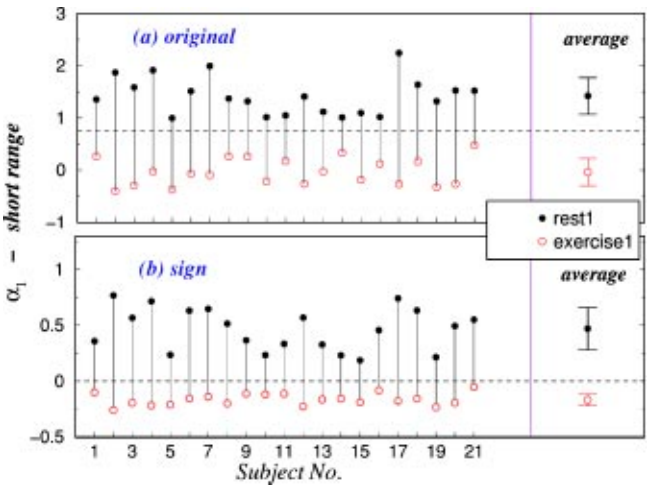

FIG. 3. Short-range scaling exponents α_1 from 21 healthy individuals (a) for the original IPI series and (b) for the sign series at rest (●) and during exercise (○). At the right hand side we show the average $\alpha_1 \pm$ standard deviation. In accordance with Fig. 2, the short-range exponents during exercise are significantly smaller than during rest. Note the complete separation of the two stages, emphasized by the dashed lines.

tion function exponent γ [$C(n) \sim n^{-\gamma}$ when $0 < \gamma < 1$] and to the power spectrum exponent β ($S(f) \sim 1/f^{\beta}$) by $\alpha = 1 - \gamma/2 = (\beta+1)/2$ [13]. The value $\alpha = 0.5$ indicates that there are no (or finite-range) correlations in the data. When $\alpha < 0.5$ the series is *anticorrelated*, meaning that large values are most probable to be followed by small values. When $\alpha > 0.5$ the series is *correlated*, meaning that large values are most probable to be followed by large values. The higher the α is, the stronger are the correlations in the signal.

We also study the correlation properties of the sign series, sgn(Δu_i) [14], derived from the IPI increments $\Delta u_i = u_{i+1} - u_i$ [15]. The simplicity of the sign series may allow easier interpretation of the results. Figs. 1(c) and 1(d) show representative examples of sign series obtained from rest and exercise stages, respectively. For exercise, the signs of IPI increments tend to alternate rapidly, indicating a strong anticorrelated behavior. At rest stage, on the other hand, the signs alternate every several points, and thus this dynamics may be characterized by a randomlike behavior at small scales.

Due to the fact that during exercise the IPI series exhibits strong short-range anticorrelations, we first integrate the IPI series for all rest and exercise episodes (in addition to the integration builtin the DFA method), to avoid inaccurate estimation of the scaling exponents for exercise segments. Because of the apparent linear decrease of the IPI during the exercise stage [Fig. 1(b)], the extra integration introduces a parabolic trend. To eliminate the effect of this parabolic trend in the exercise stage, we perform third order DFA [16] on the *integrated* IPI series. The integration procedure is not necessary for evaluating α for the rest episodes, since they exhibit correlated behavior [17].

In Fig. 2(a) we present the fluctuation function $F(n)$ of the integrated IPI series [18] for rest and exercise segments of a typical subject. For all 21 individuals we observe a characteristic crossover around $n \approx 20$, where there is a change in the correlation behavior between short- and intermediate-scales regimes. We denote the scaling exponent of the short-range regime as α_1 (estimated for scales $8 \leqslant n \leqslant 14$) and the scaling exponent of the intermediate regime as α_2 (estimated for $30 \leqslant n \leqslant 300$) [19]. The type of crossover is different for rest and exercise: for the rest $\alpha_1 > \alpha_2$, while for the exercise $\alpha_1 < \alpha_2$. The fluctuation functions for rest and exercise stages construct a ''fish''-like pattern (Fig. 2).

We apply a similar scaling analysis to sign series derived from rest and exercise segments of the IPI series [Fig. 2(b)]. The sign series do not have any global trend, thus, in this case it is enough to use second order DFA. For sign series we calculate the short-range scaling exponent α_1 in the range $6 \leqslant n \leqslant 12$ and intermediate exponent α_2 in the range $20 \leqslant n \leqslant 60$ [20].

We obtain a very good separation between rest and exercise for the original and sign series in both the short-range and the intermediate-range regimes (see Fig. 3 and Table I). The *p values* for the original and sign series (obtained by the paired samples student's *t test* [21]) are less than 10^{-10} for the short-range regime and less than 10^{-4} for the intermediate regime. The fact that sign series behave similarly to IPI series may indicate that in many cases only the direction of an increment is of import, and not the magnitude. We find that our results are robust and do not change significantly for the second rest-exercise episode (Table I).

To illustrate the importance of considering separately rest and exercise episodes, we perform our analysis also on the entire IPI records which include rest and exercise episodes altogether [Fig. 1(b)]. We find indeed that the scaling of the whole record reflects neither the correlation properties of rest, nor of exercise (see Table I).

TABLE I. Comparison of scaling exponents α_1 and α_2 between rest stages, exercise stages, and whole records that include rest and exercise episodes all together. For each stage the average scaling exponent ± standard deviations are shown.

	Original IPI series		Sign of IPI increments	
	α_1	α_2	α_1	α_2
Rest 1	1.42±0.35	0.78±0.16	0.47±0.19	0.17±0.11
Rest 2	1.43±0.30	0.75±0.17	0.38±0.26	0.15±0.12
Ex. 1	−0.04±0.26	1.07±0.18	−0.17±0.05	0.41±0.09
Ex. 2	−0.14±0.17	1.11±0.16	−0.21±0.06	0.41±0.1
Whole	1.21±0.25	0.91±0.12	0.23±0.15	0.22±0.07

The significant differences between the values of α_1 (Fig. 3) and the different crossover patterns for rest and exercise stages (Fig. 2) may offer insight on the underlying physiological mechanism controling the heartbeat dynamics. The heart rhythm is regulated mainly by the parasympathetic (PS) and the sympathetic (SM) branches of the autonomic nervous systems [22]. PS impulses slow the heart rate while SM impulses accelerate it. The interaction between these two branches is reflected by the time organization of the IPI series [Fig. 1(b)].

In a recent work Ivanov *et al.* [23] proposed a general approach based on the concept of stochastic feedback to account for the complex time organization in biological rhythms. In this framework the time evolution of a physiologic system, e.g., the heartbeat dynamics, can be represented by a random walk biased toward some preferred ''attracting'' levels. Both the SM and PS systems controlling the heart rhythm generate attracting levels which bias the walker (modelling the interbeat interval series) in opposite directions leading to complex heartrate fluctuations. Although these attracting levels change in time, according to the response of the intrinsic physiological mechanism, they can vary in a limited range only, thus keeping the walker away from extreme values.

Based on this general approach we suggest an intuitive schematic scenario that might contribute to a better understanding of different crossover patterns of the IPI fluctuations for rest and exercise (Fig. 2). At rest both the SM and PS systems are active, and each of them attracts the walker toward its own level [Fig. 4(a)]. When the walker is between the two attracting levels, each level imposes a bias in an opposite direction, practically canceling the effect of one another. Thus the walker is free to move in both directions until he crosses any of the two levels after which he is pulled back. This picture reproduces the crossover in the scaling behavior (Fig. 2) from a larger value of the correlation exponent at short scales, where the fluctuations of the walker are not bounded, to a lower value of the exponent at large-time scales, where the dynamics of the walker is limited by the SM and PS attracting levels.

During exercise the SM system dominates [25], and the dynamics can be described effectively by a single attracting level [Fig. 4(b)]. In this case the walker fluctuates around this level producing an anticorrelated behavior at short-time scales. However, since the attracting level changes with time and since the walker follows these changes, the fluctuations in the walk increase at intermediate time scales, causing a crossover to a more correlated behavior (Fig. 2).

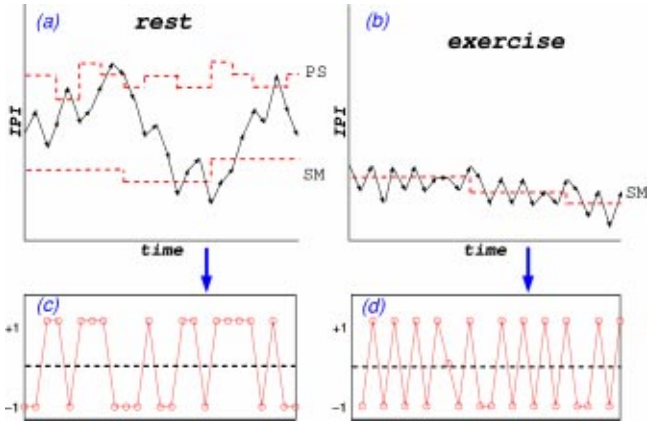

FIG. 4. Schematic illustration of a random walk with (a) two different levels of attraction and (b) a single attraction level, and their sign decomposition (c) and (d). (a) At rest the combined effect of the upper level [representing the parasympathetic (PS) system] and the lower level [sympathetic (SM) system] [24] does not restrict the walker's fluctuations as long as the walker is between the two attracting levels. But whenever the walker crosses any of them, he is immidiately pulled back. (b) On the other hand, during exercise the walker attracted by a single SM level cannot get far away from the attractor, resulting in smaller fluctuations compared to rest. The sign series for the two attractive levels presented in (c) is more likely to cluster than the series for a single level scenario presented in (d) [compare with sign dynamics for rest and exercise shown in Fig. 1(c) and Fig. 1(d)].

This schematic scenario may also provide a qualitative explanation of the remarkable differences in the amplitude of fluctuations at rest and during exercise [see Fig. 1(b)]. When the walker is between the two attracting levels no total force is acting at him, thus he has a finite probability to go several steps in the same direction [Fig. 4(c)]. On the other hand, for the case of a single attracting level, there is a strong constraint forcing the walker to change his direction [Fig. 4(d)]. That is why at rest when both levels are active the fluctuations are larger compared to exercise when there is a single dominant attracting level.

Our findings can be supported by other studies, comparing the heartbeat dynamics of healthy people and congestive heart failure patients. For heart failure patients there are evidences of a reduced vagal tone (PS activity) [26], resembling the state of the autonomic nervous system under physical exercise when SM system dominates. Indeed, heart failure patients possess decreased variability of heartbeat fluctuations compared to normal conditions [27] and a similar crossover pattern, but with different scaling exponents [8].

In summary, we study correlations in heartbeat fluctuations and show significant differences in scaling patterns between rest and exercise. We also suggest a schematic scenario in an effort to provide an intuitive explanation of our results from physiological point of view. Although this

speculative scenario should not be treated as a real model coming to explain all the complexity of heartbeat dynamics, we believe it may contribute to a better understanding of the mechanism underlying heartbeat fluctuations.

We wish to thank J.W. Kantelhardt and J.M. Hausdorff for helpful discussions. This work was supported by the Binational Israel-USA Science Foundation and the NIH/National Center for Research Resources (Grant No. P41 RR13622).

[1] J.B. Bassingthwaighte, L.S. Liebovitch, and B.J. West, *Fractal Physiology* (Oxford University Press, Oxford, 1994).
[2] M.F. Shlesinger, Ann. N.Y. Acad. Sci. **504**, 214 (1987).
[3] C.-K. Peng *et al.*, Phys. Rev. Lett. **70**, 1343 (1993).
[4] P.Ch. Ivanov *et al.*, Nature (London) **383**, 323 (1996).
[5] H.V. Huikuri *et al.*, Circulation **101**, 47 (2000); Y. Ashkenazy *et al.*, Europhys. Lett. **53**, 709 (2001).
[6] Database provided by Itamar Medical Ltd. (Cesarea, Israel), http://www.itamar-medical.com.
[7] R.P. Schnall *et al.*, Sleep **22**, 939 (1999).
[8] C.-K. Peng *et al.*, Chaos **5**, 82 (1995).
[9] P.Ch. Ivanov *et al.*, Europhys. Lett. **48**, 594 (1999).
[10] C.-K. Peng *et al.*, Phys. Rev. E **49**, 1685 (1994).
[11] First order DFA filters out constant trends in the time series, second order DFA filters out linear trends, etc.
[12] A. Bunde *et al.*, Phys. Rev. Lett. **85**, 3736 (2000).
[13] T. Vicsek, *Fractal Growth Phenomenon*, 2nd ed. (World Scientific, Singapore, 1993), pp. 38-40.
[14] Y. Ashkenazy *et al.*, Phys. Rev. Lett. **86**, 1900 (2001); Y. Ashkenazy *et al.*, e-print cond-mat/0111396.
[15] If, due to finite resolution, $\Delta u_i = 0$, we define $\mathrm{sgn}(\Delta u_i) = 0$.
[16] We find similar scaling exponents using fourth order DFA. This indicates that we have reached the ''real'' scaling which is not an artifact of a global trend during exercise.
[17] We applied DFA directly on nonintegrated IPI series at rest and found that the results are very close to those obtained using the extra integration (see Ref. [18] for details).
[18] We denote α as the scaling exponent for the original nonintegrated series. The integration of a series increases the value of α by 1. Thus, we normalize the fluctuation function of the *integrated* IPI series $\tilde{F}(n)$ by the window size n, to restore the original α, $F(n) \equiv \tilde{F}(n)/n \sim \tilde{n^{\alpha}}/n \sim n^{\alpha+1}/n \sim n^{\alpha}$.
[19] The range of window sizes is chosen to exclude the crossover region, where there is a continuous change in the scaling behavior.
[20] The differences in ranges of scaling exponents between original IPI and sgn(Δ IPI) are due to a shift in the scaling pattern, caused by applying a higher order DFA. For large-time scales sign series become uninformative indicating an uncorrelated behavior [14], making us limit the upper boundary of the intermediate range to 60 beats.
[21] W.H. Press, S.A. Teulkovsky, W.T. Vetterling, and F.P. Flannery, *Numerical Recipies in C*, 2nd ed. (Cambridge University Press, Cambridge, 1996), pp. 615–618.
[22] R.M. Berne and M.N. Levy, *Cardiovascular Physiology*, 8th ed. (Mosby, St. Louis, 2000), pp. 85–97.
[23] P.Ch. Ivanov *et al.*, Europhys. Lett. **43**, 363 (1998).
[24] The attracting level of the PS system alters more rapidly than that related to the SM system due to the difference in the response times between the two systems [22,23].
[25] B.F. Robinson *et al.*, Circ. Res. **19**, 400 (1966).
[26] J.P. Saul *et al.*, Am. J. Cardiol. **61**, 1292 (1988).
[27] C.-S. Poon and C.K. Merril, Nature (London) **389**, 492 (1997).